THE JOURNAL OF PHYSICAL CHEMISTRY Letters

Letter

pubs.acs.org/JPCL

Determining Drug Efficacy Using Plasmonically Enhanced Imaging of the Morphological Changes of Cells upon Death

Mena Aioub, Lauren A. Austin, and Mostafa A. El-Sayed*

Laser Dynamics Laboratory, School of Chemistry and Biochemistry, Georgia Institute of Technology, 901 Atlantic Drive, Atlanta, Georgia 30332-0400, United States

Supporting Information

ABSTRACT: Recently, we utilized the optical properties of gold nanoparticles (AuNPs) for plasmonically enhanced Rayleigh scattering imaging spectroscopy (PERSIS), a new technique that enabled the direct observation of AuNP localization. In this study, we employ PERSIS by using AuNPs as light-scattering probes to compare the relative efficacy of three chemotherapeutic drugs on human oral squamous carcinoma cells. Although the drugs induced apoptotic cell death through differing mechanisms, morphological changes including cell membrane blebbing and shrinkage, accompanied by an increase in white light scattering, were visually evident. By utilizing the AuNPs to increase the cells' inherent Rayleigh scattering, we have obtained the time profile of cell death from the anticancer drugs using a single sample of cells in real time, using inexpensive equipment available in any lab. From this time profile, we calculated cell death enhancement factors to compare the relative efficacies of the different drugs using our technique, which corresponded to those calculated from the commonly used XTT cell viability assay. Although this technique does not impart molecular insights into cell death, the ability to quantitatively correlate cell death to morphological changes suggests the potential use of this technique for the rapid screening of drug analogues to determine the most effective structure against a disease or cell line.

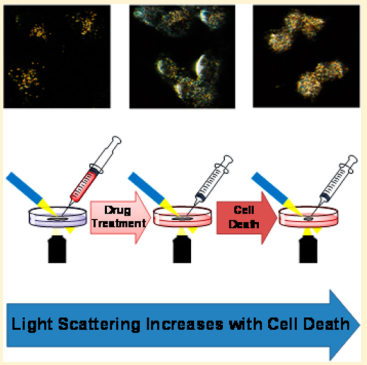

SECTION: Plasmonics, Optical Materials, and Hard Matter

Plasmonic nanoparticles have been heavily utilized in the biomedical field due to their small size and unique physical, optical, and chemical properties.[1−4] In particular, the plasmonically enhanced scattering of gold nanoparticles (AuNPs) has been used in cellular imaging applications to differentiate cancerous from noncancerous cells[5] and in surface-enhanced Raman spectroscopy to observe the molecular dynamics of apoptosis[6] and to detect biomarkers in complex physiological environments.[7] We recently developed a new technique, plasmonically enhanced Rayleigh scattering imaging spectroscopy (PERSIS), which enabled cellular imaging and the observation of AuNP localization. The AuNP localization caused a change in the intensity and the wavelength of light scattered by the nanoparticles as they came into close proximity.[8] Here, we utilize this technique, specifically the change in scattering intensity, to study the relative efficacy of three anticancer drugs (cisplatin, camptothecin, and 5-fluorouracil (5-FU)) in human oral squamous carcinoma (HSC-3) cells. This technique is validated against a commercially available XTT cell viability assay.

Normal progression through the cell cycle plays a critical role in the health and proliferation of living cells. Perturbations in this cycle can cause the loss of essential cellular functions or unwanted mutations, necessitating safeguards such as apoptosis, which results in the programmed death of cells that have mutated (i.e., become malignant) or lost vital functions.[9] Not surprisingly, many anticancer drugs attempt to induce apoptosis in these malignancies, often by disrupting DNA synthesis or replication.[10−12] However, the precise mechanism of action differs between drugs, leading to fluctuations in efficacy based on the cells' current phase in their replication cycles. For example, camptothecin inhibits DNA topoisomerase I, making it most effective during the S-phase,[13] whereas cisplatin forms DNA cross-link adducts leading to increased cellular sensitivity in the G1-phase,[14] and 5-FU blocks DNA synthesis by inhibiting thymidylate synthase and incorporation into RNA, causing G1/S-phase arrest.[15] Despite the differing mechanisms of action for these drugs, the morphological characteristics of apoptotic cell death are retained, specifically cell shrinkage, membrane blebbing, and enhanced white light scattering due to the aggregation of cellular components.[12]

To monitor the light scattering and morphology of treated cells, AuNPs were used as light-scattering probes to enhance the cells' inherent Rayleigh scattering. PERSIS experiments were conducted in a live-cell chamber (Figure 1A) to obtain both Rayleigh scattering dark-field images and Rayleigh scattering spectra from single cells incubated with AuNPs. The temporal effect of drug treatment was monitored via changes in the scattering spectra following drug administration. We have previously shown that the surface chemistry of AuNPs

Received: September 3, 2014
Accepted: September 29, 2014
Published: September 29, 2014

   dx.doi.org/10.1021/jz501866g | J. Phys. Chem. Lett. 2014, 5, 3514−3518

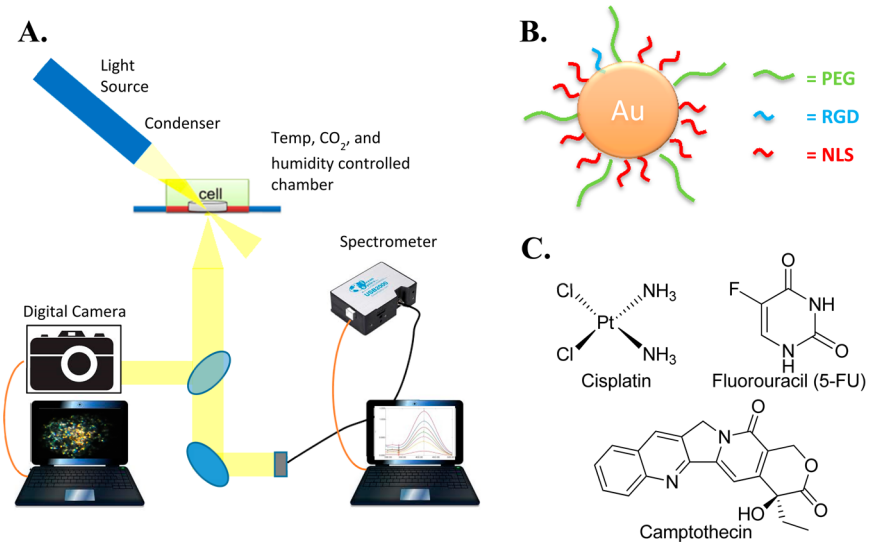

Figure 1. (A) Schematic of the PERSIS instrument used to monitor drug efficacy. (B) Illustration of the NT-AuNPs used to enhance the Rayleigh scattering. (C) Chemical structure of the anticancer drugs used.

dictates their localization within cells and, consequently, is responsible for their observed strong light-scattering properties.[8] Thus, we used nuclear-targeted AuNPs (NT-AuNPs, Figure S1, Supporting Information) for their greater light-scattering abilities. Citrate-capped AuNPs were synthesized, and their surfaces were modified to contain polyethylene glycol (PEG) to increase biocompatibility and prevent nonspecific interactions under physiological conditions.[16,17] After PEGylation, arginine-glycine-aspartic acid (RGD) and nuclear localizing sequence (NLS) peptides were bioconjugated to the AuNPs' surfaces (Figure 1B). RGD was used to increase nanoparticle endocytosis by targeting $\alpha\beta$ integrins on the cell membrane,[18,19] while NLS was used to selectively target the AuNPs at the cell nuclei[20,21] and to increase scattering by localizing the plasmonic nanoparticles. HSC-3 cells were chosen as the model cell line due to the overexpression of $\alpha v\beta 6$ integrins on their membrane.[22] To validate our technique, we calculated the time required to reach a half-maximal increase in scattering intensity, which is indicative of apoptosis. The relative drug efficacies obtained using our technique compared favorably to those obtained using the commercial XTT cell viability assay.

Determining Nanoprobe Pretreatment. The life cycle of a dividing cell has been extensively characterized from the G1-phase, which includes cell growth and preparation for DNA replication in the forthcoming S-phase through the G2-phase, which comprises the preparation for mitosis and the birth of two daughter cells in the M-phase.[23] To effectively compare the relative efficacy of several anticancer drugs, the concentration of AuNP scattering probes must be chosen to enhance scattering without affecting normal cellular function (e.g., altering the cell cycle) or inducing cell death. Accordingly, flow cytommetry was used to evaluate the effect of AuNP pretreatment on the distribution of cells throughout various stages of the cell cycle. As shown in Figure S2 (Supporting Information), no significant changes were observed in the cell cycle upon treatment with low concentrations of NT-AuNPs (0.1 and 0.2 nM) relative to the untreated control cells. Thus, pretreatment with low concentrations of NT-AuNPs is not expected to affect anticancer drug treatment, allowing AuNPs to be used as scattering probes for the effective evaluation of relative drug efficacies. Both 0.1 and 0.2 nM NT-AuNPs gave similar scattering enhancement upon cell death (~50%); therefore, 0.1 nM was used for the remaining experiments.

Drug Efficacy via Cell Viability Assays. In order to assess the validity of our PERSIS technique to the current assay standard, the efficacies of three popular anticancer drugs, cisplatin, camptothecin, and 5-FU (Figure 1C), were first determined. Efficacy was expressed as the effective time needed to induce 50% cell death (ET_{50}) following treatment with the anticancer drugs. To mimic the conditions of the PERSIS experiments, cells were first pretreated with 0.1 nM NT-AuNPs in culture media for 24 h. The AuNP solutions were then replaced with 100 μM solutions of the anticancer drugs for the desired treatment times. We obtained the temporal response of cancer cell viability to anticancer drug treatment over 72 h using an XTT cell viability assay (Figure 2). These time profiles showed the enhanced efficacy of cisplatin (ET_{50} = 16 ± 1 h) relative to camptothecin and 5-FU, which had ET_{50} values of 52 ± 3 and 67 ± 2 h, respectively. For a simpler comparison between the drugs, we used the previously established cell death enhancement (CDE) factor,[24] which is defined as the ratio of the ET_{50} values of camptothecin or 5-FU relative to cisplatin. Using the ET_{50} values extracted from the curve fits of the cell death time profiles in Figure 2, CDE factors were calculated to be 3.3 for camptothecin and 4.2 for 5-FU. Additionally, treatment with NT-AuNPs alone did not induce any significant cell death (Figure 2), further indicating that the low concentration of AuNPs served only to enhance Rayleigh scattering from the cells, allowing for greater differentiation between dead cells and living cells, without affecting cellular function or drug treatment.

Drug Efficacy via PERSIS Technique. To compare drug efficacies using our PERSIS technique, cells were pretreated with 0.10 nM NT-AuNPs for 24 h to enhance their Rayleigh scattering. The AuNP solutions were then replaced with 100 μM solutions of the anticancer drugs, and cellular morphology and light scattering were monitored from 10 different cells for 24 h via Rayleigh scattering spectra (Figure 3) and dark-field images (Movies S1–S4, Supporting Information). After drug administration, the Rayleigh scattering spectra initially remained constant but increased over time as cell death

dx.doi.org/10.1021/jz501866g | J. Phys. Chem. Lett. 2014, 5, 3514–3518

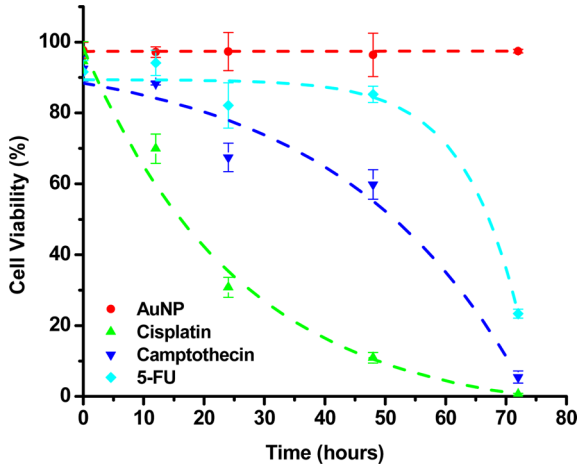

Figure 2. Time profile of HSC-3 cells treated with 100 μM cisplatin (green), camptothecin (blue), and 5-FU (teal), shown as the average cell viability ± s.e.m. from three independent experiments. ET_{50} values were calculated to be 16 ± 1 h for cisplatin (R^2 = 0.976), 52 ± 3 h for camptothecin (R^2 = 0.977), and 67 ± 2 h for 5-FU (R^2 = 0.981), giving CDE factors of 3.3 and 4.2 for camptothecin and 5-FU, respectively. Control cells treated with AuNPs alone (red) did not have a significant decrease in viability.

progressed. As seen in Figure 3, cisplatin induced the quickest increase in Rayleigh scattering, while 5-FU treatment displayed the slowest scattering increase. These trends correlate well with that previously observed using XTT cell viability assays. Complete cell death was signified when the spectra remained constant and changes were no longer observed. Dark-field images were also taken and combined into movies for the control cells that did not receive drug treatment (Movie S1, Supporting Information), and cells treated with cisplatin, camptothecin, and 5-FU (Movies S2–S4, Supporting Information, respectively), which allowed the cell death to be observed visually. Upon drug treatment, the initially viable cells were seen to first shrink and lose mobility, indicative of apoptosis,[12] and then showed a large increase in light scattering due to having more nanoparticles in close proximity.[25,26] Thus, the number of nanoparticles with optimal interparticle separation distances increased within the shrunken cells, resulting in greater scattering intensities. Eventually, the cell morphology remained constant, and the treated cells ceased all movement. It should be noted that the number of visible cells decreased as some of the dead cells floated off of the culture dish and out of the focal plane of the microscope. HSC-3 cells that did not receive anticancer drug treatment did not exhibit these visual changes and were seen to increase in number due to cell cycle proliferation.

To quantitatively compare the relative efficacy of the anticancer drugs using the PERSIS technique, the time profile of cell death was obtained to correlate the observed visual changes and increased light scattering to the biochemically

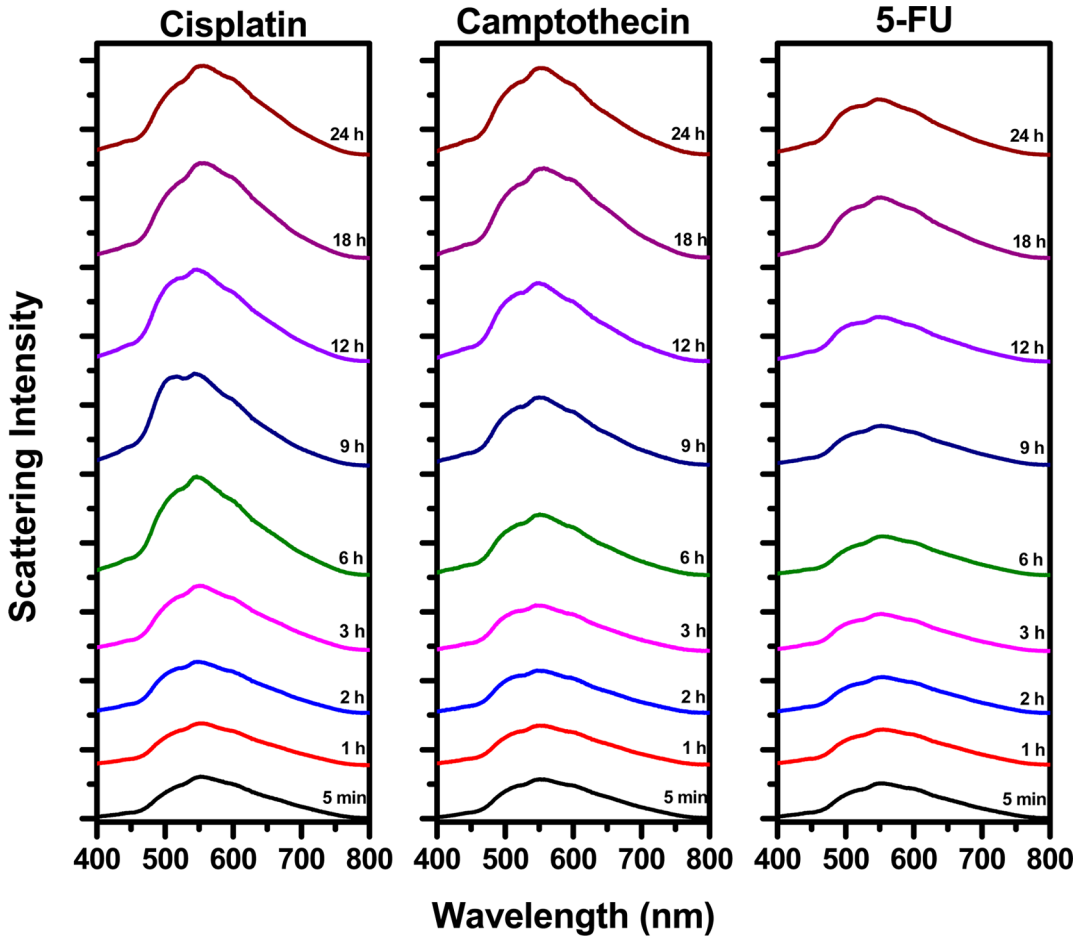

Figure 3. Real-time Rayleigh scattering spectra of HSC-3 cells treated for 24 h with 100 μM cisplatin, camptothecin, and 5-FU, shown as the mean ± s.e.m. of three independent experiments (n = 10 cells).

dx.doi.org/10.1021/jz501866g | J. Phys. Chem. Lett. 2014, 5, 3514–3518

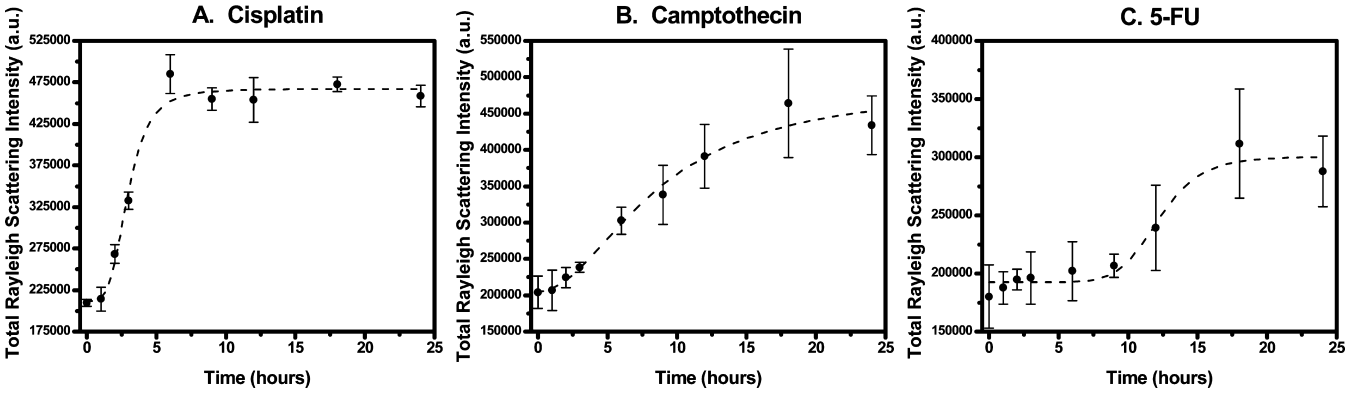

Figure 4. Rayleigh scattering intensity time profiles of HSC-3 cells treated with 100 μM cisplatin, camptothecin, and 5-FU, shown as the average intensity ± s.e.m. from three independent experiments. Scattering half-times were calculated to be 2.9 h for cisplatin (A, R^2 = 0.982), 8.6 h for camptothecin (B, R^2 = 0.976), and 12 h for 5-FU (C, R^2 = 0.928), giving CDE factors of 3.0 and 4.1, respectively.

determined cell death parameters. The Rayleigh scattering spectra in Figure 3 were integrated to obtain the total scattering intensity. These intensities, shown in Figure 4, were plotted temporally to obtain a time profile of cell death based on the increased light scattering from the cells upon drug treatment. The plasmonically enhanced Rayleigh scattering was found to initially remain constant for all of the samples, before a large increase due to cell death. However, the scattering profiles changed at different rates, which correlated with the differences observed in the ET_{50} values obtained using the XTT cell viability assay. Additionally, NT-AuNP incubated cells that were not treated with anticancer drugs did not display any significant changes in scattering over 24 h, as seen in Figure S3 (Supporting Information). To effectively compare these changes, scattering half-times, defined as the time required to achieve the half-maximal increase in scattering intensity, were calculated for each drug (details in the Supporting Information). Cisplatin had the fastest scattering half-time of 2.9 ± 0.2 h, followed by camptothecin and 5-FU with scattering half-times of 8.6 ± 1.6 and 12 ± 0.8 h, respectively (Figure 4). These scattering half-times are again similar to the trends observed from the biochemically determined drug efficacies (Figure 2). To directly compare drug efficacies as well as compare our PERSIS technique with traditional cell viability assays, we calculated CDE factors for the anticancer drugs using the ratio between the scattering half-times of camptothecin or 5-FU relative to cisplatin. As shown in Table 1, the CDE factors for camptothecin (3.0) and 5-FU (4.1) calculated using the PERSIS technique compared favorably to those obtained using the XTT cell viability assay (3.3 and 4.2, respectively), indicating the ability of PERSIS to accurately assess drug efficacy. Moreover, the PERSIS technique, including nanoparticle pretreatment, decreased the time required to obtain ET_{50} values by 24 h.

Table 1. CDE Factors Obtained Using the PERSIS Technique, Comparable to Those Obtained Using a Standard XTT Cell Viability Assay

drug	XTT ET_{50} (h)	PERSIS ET_{50} (h)	CDE factor (XTT)	CDE factor (PERSIS)
cisplatin	16 ± 1	2.9 ± 0.2		
camptothecin	52 ± 3	8.6 ± 1.6	3.3	3.0
5-FU	67 ± 2	12 ± 0.8	4.2	4.1

In conclusion, we have demonstrated the accuracy of our PERSIS technique for determining relative drug efficacies using NT-AuNPs as scattering enhancement probes. The model cell line, HSC-3, was pretreated with a low concentration of AuNPs to enhance their Rayleigh scattering without affecting normal cellular function or inducing cell death. The relative drug efficacies obtained with our technique correspond favorably to those obtained using a standard cell viability assay. The PERSIS technique presents a novel system for studying the effects of drug treatment based on the morphological changes and increase in scattered light observed upon cell death. This represents a continuous assay capable of monitoring a single sample of living cells in real time, without the need for expensive instrumentation. Furthermore, this home-built system has the potential to be engineered into a multicomponent assay capable of screening multiple samples simultaneously, which could allow for the rapid comparison of various drugs, or drug analogues, against a particular disease or cell line.

■ ASSOCIATED CONTENT

Supporting Information

Gold nanoparticle TEM and UV−vis spectra, cell cycle analysis, detailed methods, and cell death movies are included. This material is available free of charge via the Internet at http://pubs.acs.org.

■ AUTHOR INFORMATION

Corresponding Author

*E-mail: melsayed@gatech.edu. Adress: Department of Chemistry and Biochemistry, Georgia Institute of Technology, 901 Atlantic Drive, Atlanta, GA, 30332-0400; Adjunct Professor: Department of Chemistry, Faculty of Science, King Abdulaziz University, Jeddah, Saudi Arabia.

Notes

The authors declare no competing financial interest.

■ ACKNOWLEDGMENTS

The authors wish to thank the support of the National Institutes of Health, National Cancer Institute under Grant No. U01CA151802. M.A. and L.A.A. also wish to thank the support of the U.S. Department of Education GAANN fellowship. The authors also thank Bin Kang for valuable discussions and help with PERSIS instrument design.

REFERENCES

(1) Dreaden, E. C.; Alkilany, A. M.; Huang, X. H.; Murphy, C. J.; El-Sayed, M. A. The Golden Age: Gold Nanoparticles for Biomedicine. *Chem. Soc. Rev.* **2012**, *41*, 2740−2779.

(2) Jain, P. K.; Huang, X. H.; El-Sayed, I. H.; El-Sayed, M. A. Noble Metals on the Nanoscale: Optical and Photothermal Properties and Some Applications in Imaging, Sensing, Biology, and Medicine. *Acc. Chem. Res.* **2008**, *41*, 1578−1586.

(3) Daniel, M. C.; Astruc, D. Gold Nanoparticles: Assembly, Supramolecular Chemistry, Quantum-Size-Related Properties, and Applications toward Biology, Catalysis, and Nanotechnology. *Chem. Rev.* **2004**, *104*, 293−346.

(4) Giljohann, D. A.; Seferos, D. S.; Daniel, W. L.; Massich, M. D.; Patel, P. C.; Mirkin, C. A. Gold Nanoparticles for Biology and Medicine. *Angew. Chem., Int. Ed.* **2010**, *49*, 3280−3294.

(5) El-Sayed, I. H.; Huang, X.; El-Sayed, M. A. Surface Plasmon Resonance Scattering and Absorption of Anti-EGFR Antibody Conjugated Gold Nanoparticles in Cancer Diagnostics: Applications in Oral Cancer. *Nano Lett.* **2005**, *5*, 829−834.

(6) Kang, B.; Austin, L. A.; El-Sayed, M. A. Observing Real-Time Molecular Event Dynamics of Apoptosis in Living Cancer Cells Using Nuclear-Targeted Plasmonically Enhanced Raman Nanoprobes. *ACS Nano* **2014**, *8*, 4883−4892.

(7) Liu, X.; Dai, Q.; Austin, L.; Coutts, J.; Knowles, G.; Zou, J. H.; Chen, H.; Huo, Q. A One-Step Homogeneous Immunoassay for Cancer Biomarker Detection Using Gold Nanoparticle Probes Coupled with Dynamic Light Scattering. *J. Am. Chem. Soc.* **2008**, *130*, 2780−2782.

(8) Aioub, M.; Kang, B.; Mackey, M. A.; El-Sayed, M. A. Biological Targeting of Plasmonic Nanoparticles Improves Cellular Imaging via the Enhanced Scattering in the Aggregates Formed. *J. Phys.Chem. Lett.* **2014**, *5*, 2555−2561.

(9) Evan, G.; Littlewood, T. A Matter of Life and Cell Death. *Science* **1998**, *281*, 1317−1322.

(10) Holohan, C.; Van Schaeybroeck, S.; Longley, D. B.; Johnston, P. G. Cancer Drug Resistance: An Evolving Paradigm. *Nat. Rev. Cancer* **2013**, *13*, 714−726.

(11) Brown, J. M.; Attardi, L. D. The Role of Apoptosis in Cancer Development and Treatment Response. *Nat. Rev. Cancer* **2005**, *5*, 231−237.

(12) Fesik, S. W. Promoting Apoptosis as a Strategy for Cancer Drug Discovery. *Nat. Rev. Cancer* **2005**, *5*, 876−885.

(13) Hsiang, Y. H.; Liu, L. F. Identification of Mammalian DNA Topoisomerase-I as an Intracellular Target of the Anticancer Drug Camptothecin. *Cancer Res.* **1988**, *48*, 1722−1726.

(14) Siddik, Z. H. Cisplatin: Mode of Cytotoxic Action and Molecular Basis of Resistance. *Oncogene* **2003**, *22*, 7265−7279.

(15) Li, M. H.; Ito, D.; Sanada, M.; Odani, T.; Hatori, M.; Iwase, M.; Nagumo, M. Effect of 5-Fluorouracil on G1 Phase Cell Cycle Regulation in Oral Cancer Cell Lines. *Oral Oncol.* **2003**, *40*, 63−70.

(16) Otsuka, H.; Nagasaki, Y.; Kataoka, K. Pegylated Nanoparticles for Biological and Pharmaceutical Applications. *Adv. Drug Delivery Rev.* **2003**, *55*, 403−419.

(17) Ghosh, P.; Han, G.; De, M.; Kim, C. K.; Rotello, V. M. Gold Nanoparticles in Delivery Applications. *Adv. Drug Delivery Rev.* **2008**, *60*, 1307−1315.

(18) Castel, S.; Pagan, R.; Mitjans, F.; Piulats, J.; Goodman, S.; Jonczyk, A.; Huber, F.; Vilaro, S.; Reina, M. RGD Peptides and Monoclonal Antibodies, Antagonists of Alpha(V)-Integrin, Enter the Cells by Independent Endocytic Pathways. *Lab. Invest.* **2001**, *81*, 1615−1626.

(19) Zitzmann, S.; Ehemann, V.; Schwab, M. Arginine-Glycine-Aspartic Acid (RGD)-Peptide Binds to Both Tumor and Tumor-Endothelial Cells in Vivo. *Cancer Res.* **2002**, *62*, 5139−5143.

(20) Escriou, V.; Carriere, M.; Scherman, D.; Wils, P. NLS Bioconjugates for Targeting Therapeutic Genes to the Nucleus. *Adv. Drug Delivery Rev.* **2003**, *55*, 295−306.

(21) Tkachenko, A. G.; Xie, H.; Liu, Y. L.; Coleman, D.; Ryan, J.; Glomm, W. R.; Shipton, M. K.; Franzen, S.; Feldheim, D. L. Cellular Trajectories of Peptide-Modified Gold Particle Complexes: Comparison of Nuclear Localization Signals and Peptide Transduction Domains. *Bioconjugate Chem.* **2004**, *15*, 482−490.

(22) Xue, H.; Atakilit, A.; Zhu, W. M.; Li, X. W.; Ramos, D. M.; Pytela, R. Role of the $\alpha v\beta 6$ Integrin in Human Oral Squamous Cell Carcinoma Growth in Vivo and in Vitro. *Biochem. Biophys. Res. Commun.* **2001**, *288*, 610−618.

(23) Voet, D.; Voet, J. G.; Pratt, C. W. *Fundamentals of Biochemistry: Life at the Molecular Level*, 4th ed.; Wiley: Hoboken, NJ, 2012.

(24) Austin, L. A.; Kang, B.; El-Sayed, M. A. A New Nanotechnology Technique for Determining Drug Efficacy Using Targeted Plasmonically Enhanced Single Cell Imaging Spectroscopy. *J. Am. Chem. Soc.* **2013**, *135*, 4688−4691.

(25) Jain, P. K.; Huang, W. Y.; El-Sayed, M. A. On the Universal Scaling Behavior of the Distance Decay of Plasmon Coupling in Metal Nanoparticle Pairs: A Plasmon Ruler Equation. *Nano Lett.* **2007**, *7*, 2080−2088.

(26) Reinhard, B. M.; Siu, M.; Agarwal, H.; Alivisatos, A. P.; Liphardt, J. Calibration of Dynamic Molecular Ruler Based on Plasmon Coupling between Gold Nanoparticles. *Nano Lett.* **2005**, *5*, 2246−2252.